

A COMPUTER SIMULATION OF LONGITUDINAL SINGLE-BUNCH EFFECTS IN ELECTRON-POSITRON STORAGE RINGS\*

P. B. Wilson and K. L. F. Bane  
Stanford Linear Accelerator Center  
Stanford University, Stanford, California 94305 U.S.A.

and

Kohtaro Satoh  
National Laboratory for High Energy Physics (KEK)  
Tsukuba, Japan

Abstract

The computer code TRACK simulates longitudinal single-bunch effects in an electron-positron storage ring. The program tracks the turn-by-turn energy and phase deviations of  $N$  superparticles, where  $N$  is 100-1000. In addition to the usual RF and lattice parameters, an input to the program is the wake potential function for the ring vacuum chamber. The program has been applied to compute bunch lengthening in SPEAR as a function of charge per bunch. Although the computed results are in qualitative agreement with measurements, there are discrepancies in some details. Possible reasons for these discrepancies are discussed.

Introduction

The present computation was stimulated by an earlier turn-by-turn tracking simulation by Renieri.<sup>1</sup> For low values of charge per bunch, Renieri found that the bunch shape computed by the simulation was in agreement with that predicted by the time-independent Fokker-Planck equation. Above a threshold charge per bunch, however, the width of the bunch distribution obtained in the simulation increased beyond that predicted by the time-independent theory. In addition, the width of the energy distribution began to increase (the energy distribution is Gaussian with  $\sigma_e$  independent of current in the time-independent theory). These results of the simulation were in agreement with the observed behavior of bunches in real storage rings, such as ADONE and SPEAR. However, Renieri's computation was limited by the fact that the wake for a simple RC element was used. We decided to extend the simulation using a more general wake potential: in particular, a wake potential appropriate to SPEAR or PEP.

Recurrence Relations

Let  $\epsilon_i(n)$  be the deviation in energy from the synchronous energy for the  $i$ th particle on the  $n$ th turn, and  $t_i(n)$  the deviation in arrival time at a reference position from the arrival time of a synchronous particle. The reference position is taken at the location of the RF cavities, which are assumed to be concentrated at one location in the ring. The synchronous energy and time are determined only by the synchrotron radiation loss per turn,  $U_0$ , and not by current-dependent losses to vacuum chamber impedances. The recurrence relations for  $t$  and  $\epsilon$  are:

$$t_i(n) = t_i(n-1) + \frac{\alpha T_0}{E_0} \epsilon_i(n)$$

$$\epsilon_i(n) = \epsilon_i(n-1) - \frac{2T_0}{\tau_e} \epsilon_i(n-1) - \frac{2T_0}{\tau_d} \bar{\epsilon}(n-1) + \dot{V} t_i(n-1)$$

$$- \frac{1}{2} \dot{V} t_i^2(n-1) + 2\sigma_{e0} \sqrt{\frac{T_0}{\tau_e}} R_i(n) - V_i(n)$$

Here,  $\alpha$  is the momentum compaction factor,  $T_0$  is the revolution time,  $E_0$  is the energy,  $\tau_e$  is the radiation damping time,  $\tau_d$  is the damping time for dipole oscillations (Robinson damping),  $\dot{V}$  is the linear RF voltage

at  $t=0$ ,  $\ddot{V}$  is the second derivative of the RF voltage at  $t=0$ ,  $\sigma_{e0}$  is the natural (zero current) rms energy spread,  $R$  is a random number such that  $\bar{R}=0$  and  $\langle R^2 \rangle = 1$ , and  $V_i$  is the beam-induced voltage seen by the  $i$ th particle. The quantities  $\dot{V}$  and  $\ddot{V}$  are given by

$$\dot{V} = \omega_{rf} \hat{V} \sin \phi_s = \omega_{rf} \hat{V} [1 - (U_0/\hat{V})^2]^{\frac{1}{2}}$$

$$\ddot{V} = \omega_{rf} \hat{V} \cos \phi_s = \omega_{rf} U_0$$

where  $\omega_{rf}$  is the RF frequency and  $\phi_s$  is the synchronous phase measured from the crest of the RF voltage wave with peak amplitude  $\hat{V}$ . The Robinson damping time is computed as described in Ref. 2. The calculation takes into account the additional damping provided by the detuning of idling cavities, and a phase offset (detuning from the cavity tuning for maximum power transfer to the beam). The beam-induced voltage is written in terms of the wake potential  $w(\tau)$ , where  $\tau$  is the distance behind the point unit charge, as

$$V_i = \frac{I_0 T_0}{N} \sum_j^{t_i > t_j} w [t_i(n-1) - t_j(n-1)]$$

Note that the sum is subjected to the causality condition  $t_i > t_j$  (i.e.,  $w(\tau) \equiv 0$  for  $\tau < 0$ ).

The Wake Potential

The wake potential is obtained from the real part of the impedance function using

$$w(\tau) = \frac{2}{\pi} \int_0^\infty Z_R(\omega) \cos \omega \tau \, d\omega \quad (1)$$

For SPEAR,  $Z_R(\omega)$  is assumed to be of the form

$$Z_R = Z_0 (\omega/\omega_0) \quad \omega < \omega_0$$

$$Z_R = Z_0 (\omega/\omega_0)^{-0.68} \quad \omega > \omega_0 \quad (2)$$

The exponent in the high frequency region was fixed by Chao and Gareyte<sup>3</sup> from data on bunch lengthening. The scale factors  $Z_0 = 9000 \, \Omega$  and  $\omega_0 = 2\pi \times 1.3 \text{ GHz}$  were fixed<sup>4</sup> by comparing measured values<sup>5</sup> of the parasitic mode loss parameter as a function of bunch length with values computed from

$$k(\sigma_t) = \frac{1}{\pi} \int_0^\infty Z_R(\omega) e^{-\omega^2 \sigma_t^2} \, d\omega \quad (3)$$

The loss parameter is defined such that  $kQ^2$  gives the energy lost to the vacuum chamber impedance by charge  $Q$ . Figure 1 shows the wake potential for the assumed SPEAR impedance function given by Eq. (2) and Fig. 2 gives the corresponding loss parameter as a function of bunch length.

Equation (3) can also be used to provide an important check on the accuracy of the simulation. By conservation of energy, the mean time deviation for the bunch distribution,  $\bar{t} = (1/Q) \int_{-\infty}^\infty t I(t) \, dt$ , must shift so that the bunch picks up exactly the energy lost to the ring impedance. Thus,  $\Delta U = kQ^2 = \dot{V} \bar{t} Q$  and

$$\bar{t} = k(\sigma_t) (Q/\dot{V}) \quad (4)$$

\* Work supported by the Department of Energy, contract DE-AC03-76SF00515.

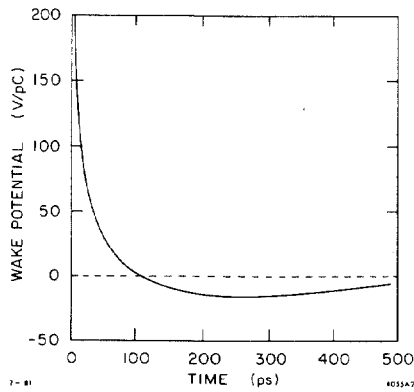


Fig. 1. Wake potential function for SPEAR.

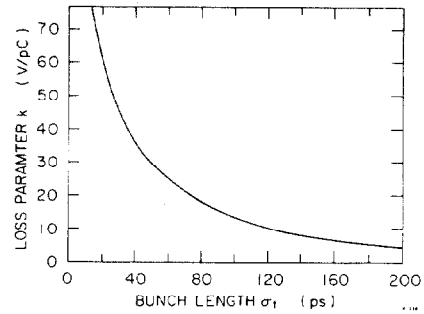


Fig. 2. Loss parameter as a function of bunch length for SPEAR.

Results for SPEAR

Figures 3-7 give an example of a run for 10,000 turns for  $N=100$  particles using the assumed SPEAR wake function. Input parameters are:  $E_0 = 2.21$  GeV,  $U_0 = 165$  keV,  $\hat{V} = 1.30$  MV,  $\alpha = 4.18 \times 10^{-2}$ ,  $T_0 = 0.781$   $\mu$ s,  $\tau_e = 10.5$  ms,  $\tau_d = 0.02$  ms,  $\omega_{rf}/2\pi = 358.5$  MHz,  $\sigma_{e0} = 1.17$  MeV and  $I_0 = 30$  mA. The program starts on turn zero with a distribution having the natural energy spread  $\sigma_{e0}$  and natural bunch length  $\sigma_{t0} = (\alpha T_0/E_0 \hat{V})^{1/2} \sigma_{e0} = 83$  ps. Figures 3 and 4 show the increase in bunch length and energy spread as a function of turn number. Note that for any turn the bunch lengthening factor  $\sigma_t/\sigma_{t0}$  and energy spread increase  $\sigma_e/\sigma_{e0}$  are equal. Figure 5 shows the mean deviation  $\bar{t}$  as a function of

turn number. It can be checked that for each turn Eq. (4) is satisfied, using Fig. 3 to obtain  $\sigma_t$  and Fig. 2 to obtain the corresponding  $k(\sigma_t)$ . The mean energy deviation  $\bar{\epsilon}$  is not shown; it oscillates about zero, as it should. Figure 6 shows bunch length oscillations for turns 9500-9600. The period is seen to be 15.5 turns, or about one-half the zero current synchrotron oscillation period (30.5 turns). Figure 7 shows a plot of the positions of the particles in phase space on turn number 9500. The dashed ellipse passes through the intercepts  $\pm\sigma_{e0}$  and  $\pm\sigma_{t0}$ , while the solid ellipse passes through  $\pm\sigma_e$  and  $\pm\sigma_t$  for turn 9500. The program will also produce histograms of the particle distributions in energy and time (bunch shape).

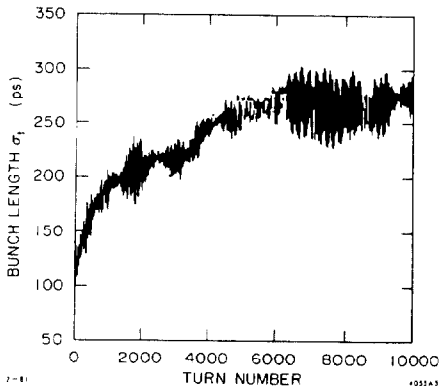


Fig. 3. Bunch length vs turn number.

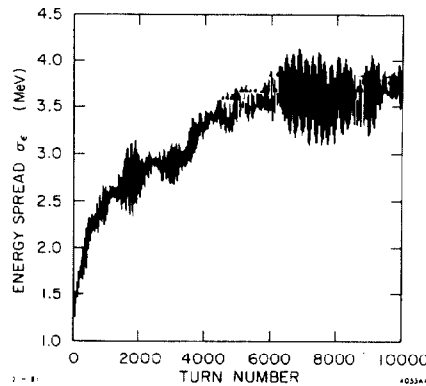


Fig. 4. Energy spread vs turn number.

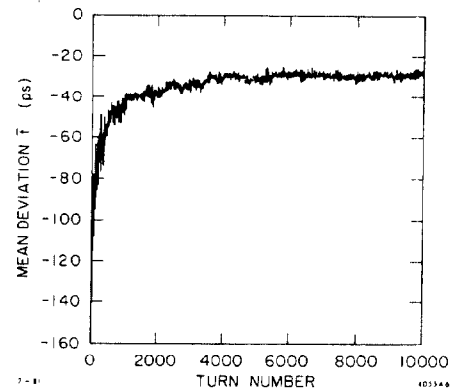


Fig. 5. Mean time deviation vs turn number.

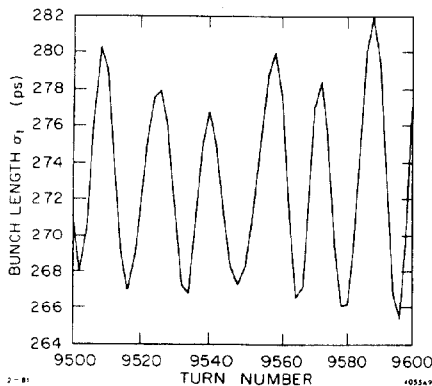


Fig. 6. Bunch length oscillations for turns 9500-9600.

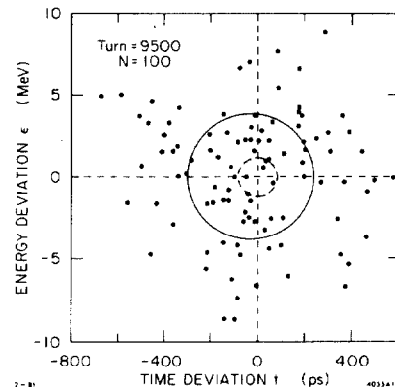


Fig. 7. Plot in phase space of 100 particles on turn 9500.

### Computed vs Measured Bunch Lengthening

Figure 8 gives a comparison of the increase in energy spread computed by this simulation with measured values<sup>5</sup> of the ratio  $\sigma_{\epsilon}/\sigma_{\epsilon_0}$ . There is qualitative

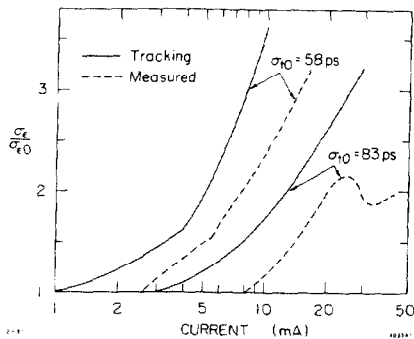


Fig. 8. Computed vs measured increase in energy spread as a function of single-bunch current.

agreement between computed values and measured data, in that both curves show a threshold current and have about the same rate of increase in  $\sigma_{\epsilon}/\sigma_{\epsilon_0}$  above threshold. However, the measured threshold is about a factor of two higher in current than the computed threshold, and the measured threshold is somewhat sharper. In addition, there is a saturation in the measured ratio for the case of  $\sigma_{t_0} = 83$  ps. Better agreement could be obtained by decreasing the amplitude of the impedance function, but this would introduce a discrepancy between computed and measured values of the loss parameter  $k(\sigma_{\epsilon})$ . Resonant buildup of higher-order RF

cavity modes could change the effective  $\dot{V}$  seen by the bunch. The threshold current for bunch lengthening is, in fact, observed to change by a substantial amount with changes in the positions of the tuners in the idling (nondriven) RF cavities. Finally, there is some evidence that there is a damping mechanism for bunch length oscillations which is not being taken into account by the program. In the real machine, the threshold for these oscillations is very sharp and coincides with the threshold for bunch lengthening.<sup>5</sup> In the simulation, the amplitude of the oscillations is not significantly lower for currents below threshold. Perhaps they are excited by a kind of shot noise, due to the rather small number of particles used in most runs ( $N=100$ ). Efforts are being made to speed up the program so that a larger number of particles can be used. The running time is proportional to  $N^2L$ , where  $L$  is the total number of turns ( $L$  must be larger than  $\tau_{\epsilon}/T_0$ ).

### References

1. A. Renieri, Laboratori Nazionali di Frascati del CNEN, Report No. LNF-75/11R (February 1976).
2. P. B. Wilson, PTM-222, Stanford Linear Accelerator Center (1980), unpublished.
3. A. W. Chao and J. Gareyte, SPEAR-197/PEP-224, Stanford Linear Accelerator Center (1976), unpublished.
4. P. B. Wilson, PEP-233, Stanford Linear Accelerator Center (1977), unpublished.
5. P. B. Wilson et al., IEEE Trans. Nucl. Sci. NS-24, No. 3, 1211 (1977).